Changes in hydrodynamics and wave energy as a result of seagrass decline along the shoreline of a microtidal back-barrier estuary

Carmine Donatelli [(1*)], Neil K. Ganju [(2)], Tarandeep Singh Kalra [(3)], Sergio Fagherazzi [(4)], Nicoletta Leonardi [(1)]

*corresponding Author: Carmine@liverpool.ac.uk

(1)   Department of Geography and Planning, School of Environmental Sciences, Faculty of Science and Engineering, University of Liverpool, Roxby Building, Chatham St., Liverpool L69 7ZT, UK

(2)   U.S. Geological Survey, Woods Hole Coastal and Marine Science Center, MA 02543, USA

(3)   Integrated Statistics, Contracted to the U.S. Geological Survey, Woods Hole Coastal and Marine Science Center, MA 02543, USA

(4)   Department of Earth and Environment, Boston University, 675 Commonwealth Avenue, Boston, MA 02215, USA

Abstract:

Seagrasses are marine flowering plants that provide key ecological services. In recent decades, multiple stressors have caused a worldwide decline in seagrass beds. Changes in bottom friction associated with seagrass loss are expected to influence the ability of estuarine systems to trap sediment inputs through local and regional changes in hydrodynamics. Herein, we document a numerical study using six historical maps of seagrass distribution in Barnegat Bay, USA, to demonstrate that reductions in seagrass coverage destabilize estuarine systems, decreasing flood-dominance in areas affected by seagrass disappearance and increasing bed-shear stress values across the entire back-barrier basin. Furthermore, we reveal how seagrass decline has considerably increased the impact of wind-waves on marsh edges between 1968 and 2009. From a comparison with a numerical experiment without submerged aquatic vegetation, we estimate that up to 40% of

the computed wave thrust on marsh boundaries can be reduced by seagrass beds and we find that the location of a seagrass patch in addition to its aerial extent plays a crucial role in this attenuation process. This study highlights the benefits of seagrass meadows in enhancing estuarine resilience and reducing marsh-edge retreat by wind-wave attack, which is recognized as a chief agent in lateral marsh loss.

Keywords: seagrass, COAWST, ecosystem services, coastal resilience, tidal asymmetry.

1. Introduction

Seagrasses are marine flowering plants that can form dense underwater meadows. They are typically found in shallow depths with sufficient light levels. Seagrasses act as ecological engineers, modifying the physical and ecological environment [e.g., Carniello et al., 2016]. For instance, by reducing sediment resuspension, seagrasses can produce adequate light conditions to stimulate their own biomass production [Dennison et al., 1993; Orth et al., 2006; Carr et al., 2010]. Furthermore by stabilizing sediments, seagrasses enhance their survival rate during extreme storm conditions [Terrados and Duarte, 2000; Madsen et al., 2001; Cardoso et al., 2004]. Seagrasses provide critical ecosystem services such as nutrient cycling, organic carbon production and export, and enhanced biodiversity [Moriarty and Boon, 1989; Koch, 2001; Waycott et al., 2009]. Unfortunately, many studies have documented a large-scale seagrass decline due to global, regional and local stressors [Cambridge et al., 1986; Short and Burdick, 1996; Orth et al., 2006]. Moreover, extreme weather events (e.g. hurricanes, tsunamis) can threaten seagrass communities through meadow uprooting and burial caused by increased sediment loads [Preen et al., 1995; Koch, 1999].

Numerous studies have assessed the role of submerged aquatic vegetation (SAV) on flow and sediment transport at small scales in laboratory conditions [Dijkstra and Uittenbogaard, 2010; Nepf, 2012]. Sediment convergence and divergence, and the ensuing erosional and depositional patterns, are largely influenced by changes in the velocity field as a consequence of flow deflection and increased friction across seagrass meadows [Fonseca et al., 1982; Koch et al., 2006, Peterson et al.,

2004]. Large horizontal velocity gradients are generally present between the vegetated and bare beds, and the vertical velocity profile presents significant discontinuities at the interface between the water column occupied by the canopy and the free flow over it [e.g., Gambi et al., 1990; Koch, 2001; Ghisalberti & Nepf, 2002]. Apart from their capacity to modify tidal currents, seagrasses influence waves [e.g., Fonseca & Cahalan, 1992]. Indeed, their ability to reduce wave energy has been recognized as an important ecosystem service [Madsen et al., 2001]; several field studies and laboratory experiments have investigated the non-linear response of their buffering function to changes in vegetation characteristics [e.g., Bouma et al., 2010; Fonseca and Cahalan, 1992; Paul and Amos, 2011].

Previous numerical modelling studies have investigated the impact of climate change and water quality on seagrass decline [Carr et al., 2010; Carr et al., 2012]. In addition, Van der Heide et al. [2007] have demonstrated how the positive feedbacks between seagrass presence and turbidity in the water column might rapidly shift seagrass habitats from a stable state with clear water and high light levels to a state with strong light attenuation and no seagrass cover [Carr et al., 2010]. However, the role of seagrass has rarely been quantified at a regional scale [Ganthy et al., 2013; Donatelli et al., 2018a; Nardin et al., 2018], and there is a paucity of studies investigating the impact of changes in seagrass extent on tidal asymmetry and wave thrust attenuation along marsh boundaries using large-scale historical seagrass distribution maps [e.g., Donatelli et al., 2018a].

In this study, we use numerical simulations to analyse how variations in seagrass coverage influence the hydrodynamics across an entire back-barrier estuary located in New Jersey, USA. Six historical seagrass coverage maps of the Barnegat Bay Little-Egg Harbor system for the period 1968-2009 have been used. We used the Coupled Ocean Atmosphere-Wave Sediment Transport (COAWST) modelling system [Warner et al., 2010] and the associated submerged aquatic vegetation model, recently implemented by Beudin et al., [2017a] to determine tidal water level fluctuations and wind-waves within the estuary in different years. Contrary to a simple drag increase parameterization [e.g., Morin et al., 2000], the new vegetation module provides a more

physically based approach to simulate the three-dimensional effect of vegetation on the mean and turbulent flow [e.g., Lapentina & Sheng, 2014; Marjoribanks et al., 2014].

In this investigation, we first focus on the separate impact of seagrass on tidal propagation and wave height; we then explore changes in shear stress and wave thrust on marsh boundaries due to the compound wave and tidal actions. Our study suggests that seagrass presence can play a key role in protecting salt marshes against wind-wave attack. We also show that seagrass presence shortens the period of flood and reduces shear stresses on the estuarine seabed, which in turn influences the capacity of estuarine systems to capture and store sediment inputs from rivers and the ocean. These outcomes are relevant for the long-term survival of coastal bays [e.g., Fagherazzi et al., 2014] and suggest that seagrass can provide significant coastal protection [Temmerman et al., 2013].

2. Study site

The Barnegat Bay-Little Harbor estuary (BB-LEH) is a shallow lagoon-type estuary located in New Jersey, USA. The back-barrier bay is approximately 70 km long with a width ranging from 2.0 to 6.5 km, and an average water depth of 1.5 m [Hunchak-Kariouk et al., 1999]. The lagoon is composed of three shallow bays (Barnegat Bay, Manahawkin Bay, and Little Egg Harbor) and is connected to the ocean through two inlets (Little Egg Inlet and Barnegat Inlet). Tides are mainly semidiurnal, with the M_2 harmonic being the dominant constituent. Offshore, the tidal amplitude is ~1 m but energy dissipation through the inlets decreases the amplitude within the bay to a minimum of 0.2 m [Aretxabaleta et al., 2014]. Circulation patterns are strongly influenced by winds [Kennish et al., 2001; Defne & Ganju, 2014].

In BB-LEH, the submerged aquatic vegetation (SAV) is characterized by two main species: *Zostera marina* and *Ruppia maritima*. As showed in recent studies [Bologna et al., 2000], seagrass coverage has decreased by 62% over the last several decades; the total loss is estimated as 2000-3000 ha in 30 years (from 1960 to 1990). The main causes of the seagrass decline are related to the shading effect of phytoplankton blooms, increased growth of epiphytic algae, and wasting disease [Bologna et al., 2000; Kennish, 2001; Kennish et al., 2007a].

The bathymetry of the model used in this study is based on the National Ocean Hydrographic Survey data [NOAA-NOS, 2012] updated with field measurements [Miselis et al., 2012]. Since the 1940s there have been negligible bathymetric changes [Defne and Ganju, 2014] and even Hurricane Sandy did not alter the estuary's bathymetry over large spatial scale [Miselis et al., 2015]. The bathymetry of the study area and historical seagrass coverage are illustrated in Figure 1 of Donatelli et al. [2019] and Figure 1 in this manuscript (Figure 1g illustrating a potential future scenario with no seagrass).

3. Methods

The hydrodynamics of the system have been simulated using the COAWST (Coupled-Ocean-Atmosphere-Wave-Sediment Transport Modeling System) modeling framework [Warner et al., 2010]. In this study, the circulation model ROMS [Shchepetkin and McWilliams, 2005; Warner et al., 2008] and the wave model SWAN [Booij et al., 1999] have been fully coupled on the same computational grid, with data exchange every 600 s. ROMS (Regional Ocean Modeling System) is a three-dimensional, free surface, finite-difference, terrain following model that solves the Reynold-Averaged Navier-Stokes (RANS) equations using the hydrostatic and Boussinesq assumptions [Haidvogel et al., 2008]. SWAN (Simulating WAves Nearshore) is a third-generation spectral wave model based on the action balance equation [Booij et al., 1999]. The model simulates the generation and propagation of wind-waves accounting for shifting in relative frequency due to variations in water depth and currents, depth-induced refraction, wave-wave interactions and dissipation (white-capping, depth-induced breaking and bottom friction). The number of interior cells is 160 x 800 in cross-bay and along-bay directions with 7 vertical layers equally spaced with cell size varying from 40 to 200 m. The model is forced at the seaward boundaries with tides, using a combination of Flather [1976] and Chapman [1985] boundary conditions; a radiation boundary condition Orlanski [1976] is prescribed on the landward boundary. The tidal constituents (K_1, O_1, Q_1, M_2, S_2, N_2, K_2, M_4 and M_6) are extracted from the ADCIRC tidal database for the North Atlantic Ocean [Mukai et al., 2002]. The model framework has been implemented and calibrated by Defne and Ganju [2014]. The model was calibrated by changing the bottom roughness coefficient to attain the best agreement between model results and water level data and water discharge measurements collected by the U.S. Geological Survey in March 2012 [Defne & Ganju, 2014]. The calibration did not include SAV-hydrodynamic feedbacks. The friction exerted by the bed on flow is computed using a bottom boundary layer formulation [Warner et al., 2008] that includes enhanced wave based apparent roughness [Madsen, 1994]. The wave thrust (the integral along the vertical of the dynamic pressure of waves) is explicitly computed by the model following Tonelli et al. [2010], and Leonardi et al. [2016]. The flow-vegetation interaction is computed using the vegetation module recently

implemented in COAWST [Beudin et al., 2017; Kalra et al., 2017]. The flow-vegetation module includes plant posture-dependent three-dimensional drag, in-canopy wave-induced streaming, and production of turbulent kinetic energy and enstrophy for the vertical mixing parameterization; the spatially averaged vegetation drag force is approximated using a quadratic drag law and the effect of plant flexibility on drag is computed using the approach of Luhar and Nepf [2011]. The selected turbulence model is the k–ε scheme which accounts for extra dissipation and turbulence kinetic energy production due to vegetation [Uittenbogaard, 2003]. Similarly, the wave dissipation due to vegetation is accounted by the model modifying the source term of the action balance equation following the formulation of Mendez and Losada [2004]. The other external contributions to wave energy such as wind, wave breaking, bottom dissipation and nonlinear waves interactions are computed as follows: i) wind energy input according to Cavalieri and Malanotte-Rizzoli [1981] and Komen et al., [1984] formulations for the linear and exponential wind growth respectively; ii) bottom friction following Madsen [1988]; iii) whitecapping following Komen et al., [1984]. An idealized wind field was used, as these numerical experiments are not intended to quantify the real wave thrust on marsh boundaries but are built with the goal to unravel the effect of seagrass loss on wave energy. Different scenarios were considered for the wind forcing characterized by winds of constant speed (5, 10 and 15 m/s) blowing from south-west and south-east (Figure 1h) for the entire simulation period. As wave action on marsh edges is strongly related to tidal level [Tonelli et al., 2010], we ran the simulations for a spring-neap tidal cycle. The temporal evolution of the study site has not been considered and the present-day morphology has been used for each year. Particularly, recent studies [e.g. Leonardi, et al., 2016a, b] show that marshes are eroding at around 0.5-2 m/year, with the highest erosion rate registered in Great Bay. The resolution of the model domain is such that morphological changes due to marsh edge erosion cannot be taken into account at these erosion rates; therefore, we focus solely on the impact of seagrass coverage on waves and tides by adopting an exploratory model approach [Murray, 2007].

Salt marsh and seagrass coverage data were derived from the CRSSA's (Center for Remote Sensing and Spatial Analysis) geographic information systems (GIS) database. Vegetation parameters are listed in Table 2 of Donatelli et al. [2019] nominally selected using Kennish et al. [2013] for guidance. Simulations are run implementing different seagrass coverages corresponding to the years 1968, 1979, 1987, 1999, 2003, 2009, and for a test case without seagrasses [1968 map, U.S. Army Corps of Engineers, 1976; 1979 map, Macomber and Allen, 1979; 1987 map, Joseph et al., 1992; 1999 map, McClain and McHale 1996; Bologna et al., 2000; 2003 and 2009 maps, Lathrop and Haag, 2011].

4. Results

From 1968 until 2009, the extent of seagrass meadows within the Barnegat Bay-Little Egg Harbor system largely declined (Figure 1, Figure 2; Table 1 in Donatelli et al. [2019]). Figure 2 shows the area colonized by seagrass as a function of water depth for each year. The impact of seagrass loss on tidal propagation was evaluated following classic harmonic analysis using T_TIDE [Pawlowicz et al., 2002], and by computing the spatial distribution of the amplitude and phase lag of the M_2 constituent within the entire back-barrier basin. For coastal areas with multiple inlets, water levels are controlled by the interaction between tidal forcing propagating from each inlet, and changes in bottom friction that can alter their relative phase. A comparison between amplitude and phase lag values for the scenario with maximum seagrass coverage (year 1979) and a scenario without seagrass reveals that the phase lag of the tidal wave coming from Great Bay and directed to Barnegat Bay decreased with seagrass removal. As a consequence, the tidal amplitude within the entire northern part of the estuary increases for the non-seagrass case, because the tidal waves from Barnegat Inlet and from Great Bay have a similar phase and become additive.

Seagrass loss also influences tidal asymmetry. Asymmetric tides are important for the transport and deposition of sediments in shallow estuaries [Aubrey and Speer, 1985]. Changes in tidal asymmetry were calculated following the formulation of Friedrichs and Aubrey [1988] and are depicted in Figure 4. The amplitude and phase ratios between the fourth-diurnal M_4 constituent and the semidiurnal M_2 constituent have been calculated. Our results suggest that seagrass meadows tend to enhance the flood dominance of the system increasing the M_4 to M_2 water level amplitude ratio, as tidal nonlinearities are enhanced.

In this study, we also evaluated the influence of seagrass beds on locally generated wind-waves for winds of 5, 10, and 15 m/s blowing from the southwest and southeast. Wind directions and speeds were chosen based on the most frequent winds (Figure 1h), with southwest winds maximizing fetch in the southern half of the estuary. Figure 5 presents the distribution of mean wave heights as a function of water depth in the non-seagrass case and for the scenarios with

maximum (year 1979) and minimum (year 2009) seagrass coverage. The mean wave height is the mean value throughout the entire simulation computed at each cell. Our results show that the presence of seagrass attenuates waves across the entire bay, although this damping effect is more limited on bare beds (Figure 6). Colored areas in Figure 5 indicate locations where some seagrass is present, while no seagrass is present in the white areas of the plot. Colored areas do not necessary have 100% seagrass coverage, and red areas have the highest seagrass presence. Figure 6 distinguishes areas with and without seagrass meadows for every depth. For areas with meadows, the reduction in wave height peaks where seagrass presence is maximum. In contrast, the reduction in wave height over bare beds is more uniform across all depths with small decreases occurring where seagrass presence is maximum as well as across transitional depth values above which no seagrass are present. Results for all wind speed values are presented in the supplementary material (Figure 3-4 in Donatelli et al. [2019]).

Seagrass loss increases the action of waves and tides at the basin bottom. The distributions of shear stresses are presented in Figure 7. The presence of seagrass largely increases the extent of basin areas with shear stress values smaller than 0.1 Pa. In addition, seagrass removal rises the lateral wave thrust exerted on marsh boundaries. The spatial distribution of wave thrust averaged throughout a spring-neap tidal cycle is depicted in Figure 8 for the non-seagrass case and for the case with maximum seagrass coverage (1979). Figure 9 shows the decrease in wave action due to seagrass presence with respect to the non-seagrass case over the last 50 years. Average wave thrust reduction in time and across the entire Bay are thus expressed in terms of percentage reduction with respect to the non-seagrass case (Figure 9). Our numerical findings suggest that in Barnegat Bay, the wave attack on marsh boundaries increased significantly between 1979 and 1987 (light blue areas in Figure 10), although, on average, a small reduction in seagrass coverage occurred (Figure 10 and Table 1 in Donatelli et al. [2019]). Though the average decrease in seagrass extent was small, seagrass loss was greater in areas sheltering the marsh boundaries (Figure 2c in Donatelli et

al. [2019]). In contrary, in the last five decades, the wave thrust increased uniformly in Manahawkin Bay (Figure 10) as the seagrass removal was uniform.

5. Discussion and conclusions

The impact of submerged aquatic vegetation on wind waves and tides within a semi-enclosed shallow lagoon system has been evaluated using the Barnegat Bay-Little Egg Harbor system as test case. The analyses are based on historical trends of seagrass distribution from 1968 to 2009; a scenario with no seagrass represents a plausible system configuration in the near future. This study has shown that seagrass decline influences tidal propagation in shallow bays with multiple inlets. Specifically, changes in bottom friction alter the relative phase between the tidal waves coming from each inlet modifying water levels within the entire estuary (Figure 3).

Tidal asymmetry in coastal embayments and estuaries is governed by the ratio of tidal amplitude to mean water depth and the ratio of intertidal storage area occupied by tidal flats and salt marshes to that of channels [Speer and Aubrey, 1985]. Previous studies have investigated the impact of tidal flat elevations [e.g., Fortunato & Oliveira, 2005] and salt marsh erosion [Donatelli et al., 2018b] on tidal propagation and asymmetry within shallow estuaries. In this study, we show that seagrass also influences tidal asymmetry. For this test case, the average increase in tidal nonlinearities due to seagrass presence (Figure 4) is higher than the one caused by an increase in intertidal storage volume due to a complete removal of salt marsh areas. The latter was explored in Donatelli et al. [2018b]. Hence, submerged aquatic vegetation might increase the flood dominance of microtidal back-barrier estuaries. Particularly, the friction due to seagrasses slows the propagation of tidal water levels around low tide relative to high tide [Dronkers, 1986], leading to longer ebb and higher velocity currents during the flood phase. Moreover, we show that increased seagrass coverage decreases bed shear stress across the entire basin (Figure 7). These findings agree with previous field measurements and numerical studies [Hansen and Reidenbach, 2012; Donatelli

et al., 2018a], which demonstrate that seagrasses reduce bottom shear stresses within and behind patches, and also impact the sediment budget of coastal bays.

Marsh loss associated with edge erosion is a major mechanism of marsh deterioration in estuaries and lagoons worldwide [Schwimmer, 2001; Barbier et al., 2008; Marani et al., 2011; Tommasini et al., 2019]. Wind-waves are recognized as the chief erosional agent and Schwimmer [2001] first suggested the existence of a relationship between wave energy and marsh retreat; subsequent studies further corroborated this finding [e.g., Marani et al., 2011; Leonardi & Fagherazzi, 2014; Leonardi, et al., 2016a, b]. Tidal levels play a key role in wind-wave attack, determining the elevation at which waves attack the marsh edge. Wave action on marsh boundaries increases with tidal elevation and then drops when the marsh is submerged [Tonelli et al., 2010]. In this study we showed, in agreement with previous researches [e.g., Nowacki et al., 2017; Beudin et al., 2017b; Nardin et al. 2018], that submerged aquatic vegetation has a local effect in dampening waves. Indeed, seagrasses strongly reduce wave heights over meadows but have a more limited effect on un-vegetated flats (Figure 6). Therefore, given a certain seagrass distribution, marsh boundaries experience a decrease in wave attack and such decrease in wave action is significantly larger for those salt marshes located next to meadows.

Our numerical results show that, over the last five decades, the wave action on salt marshes fringing the mainland in the Barnegat Bay-Little Egg Harbor estuary increased with seagrass loss. Figure 10 reveals how seagrass deterioration affected wave attack in the central and north part of the estuary and highlights how the disappearance of small SAV patches next to marsh boundaries (Table S1, Figure S2) increased the wave thrust by 35% in the period 1979-1987. These results highlight that, in terms of protection of the marsh boundary, the location of disappearing seagrasses is important.

Our research underlines how seagrass decline can decrease bay sediment storage capacity and potentially enhance salt marsh lateral erosion. Because salt marsh loss reduces the ability of shallow estuaries to retain sediments [Donatelli et al., 2018b], this might in turn promote further

deterioration of salt marshes through a positive feedback loop [e.g., Ganju et al., 2017]. The influence of seagrasses on hydrodynamics should be explored seasonally as aboveground biomass peaks during June-July and declines significantly during fall, when it becomes five times smaller [Kennish et al., 2007b, 2008; Farnsworth, 1998; Koch et al., 2009; Hansen and Reidenbach, 2013]. The capacity of meadows to influence waves changes over the year and a minimum shoot density is necessary to initiate wave attenuation [e.g., Paul & Amos, 2011]. The lack of seasonal data in our study constitutes a significant gap in the understanding of how these ecosystems can affect the stability of coastal embayments over long time scales.

Figure captions

Figure 1: Seagrass coverages (a-f) for different years, i.e. 1968, 1979, 1987, 1999, 2003 and 2009; base-case: no-SAV (g); wind rose for the area (wind station, station 44025 (LLNR 830), 40°15'3''N, 73°9'52''W). For panels a-g green areas are locations where salt marshes are present. Yellow to red shading indicates areas were seagrasses are present as sparse (red), moderate (orange) or dense (yellow). Wind rose (h).
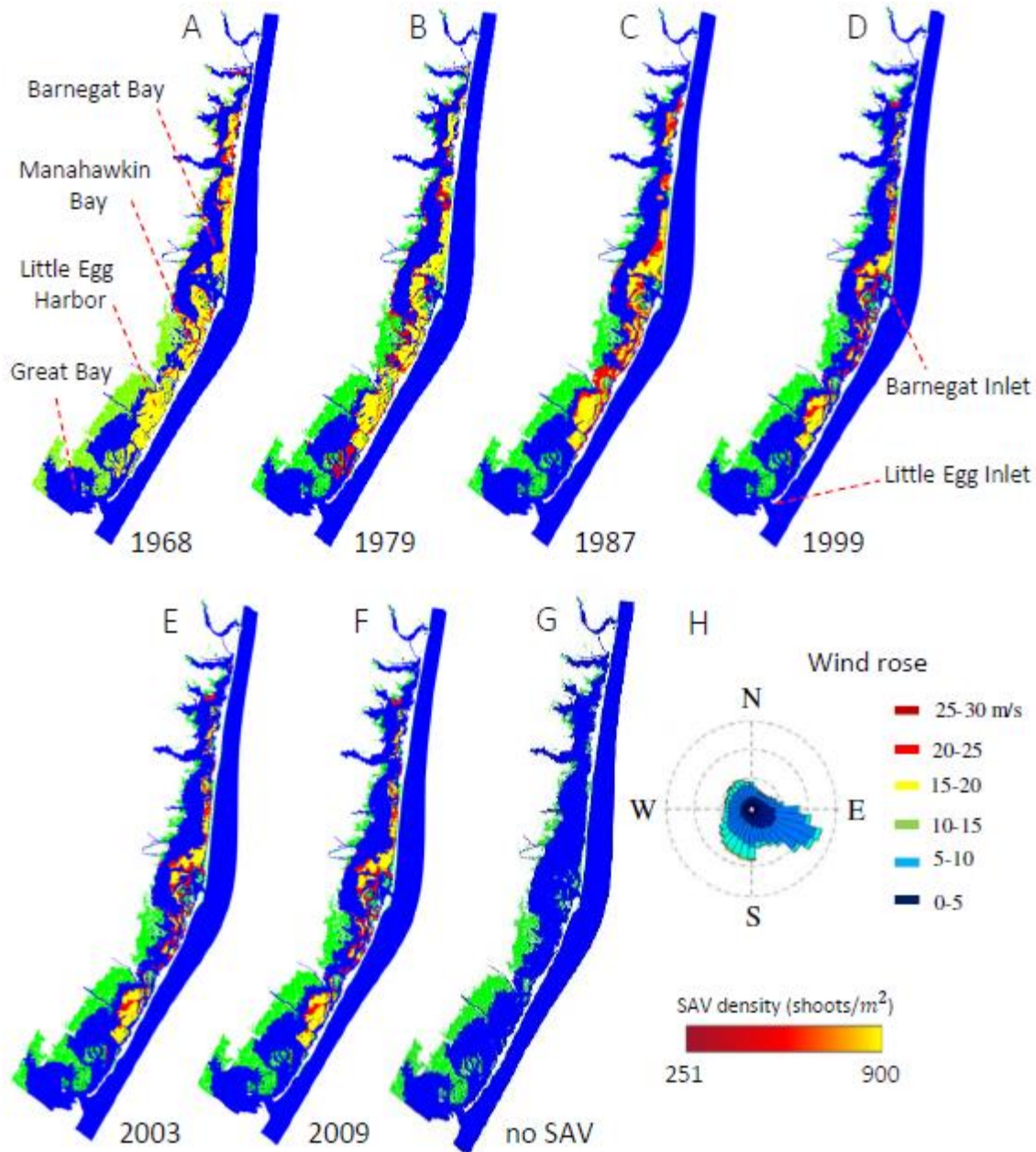
Figure 2: Area colonized by seagrass as a function of water depth for each year. Water depth data are binned every 0.15 m.
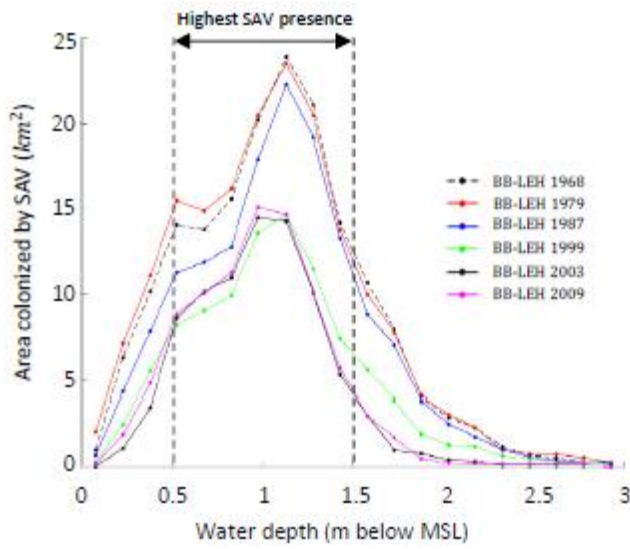
Figure 3: M_2 amplitude (cm) and phase lag (°) for year 1979 (a, c) and no SAV case (b, d).
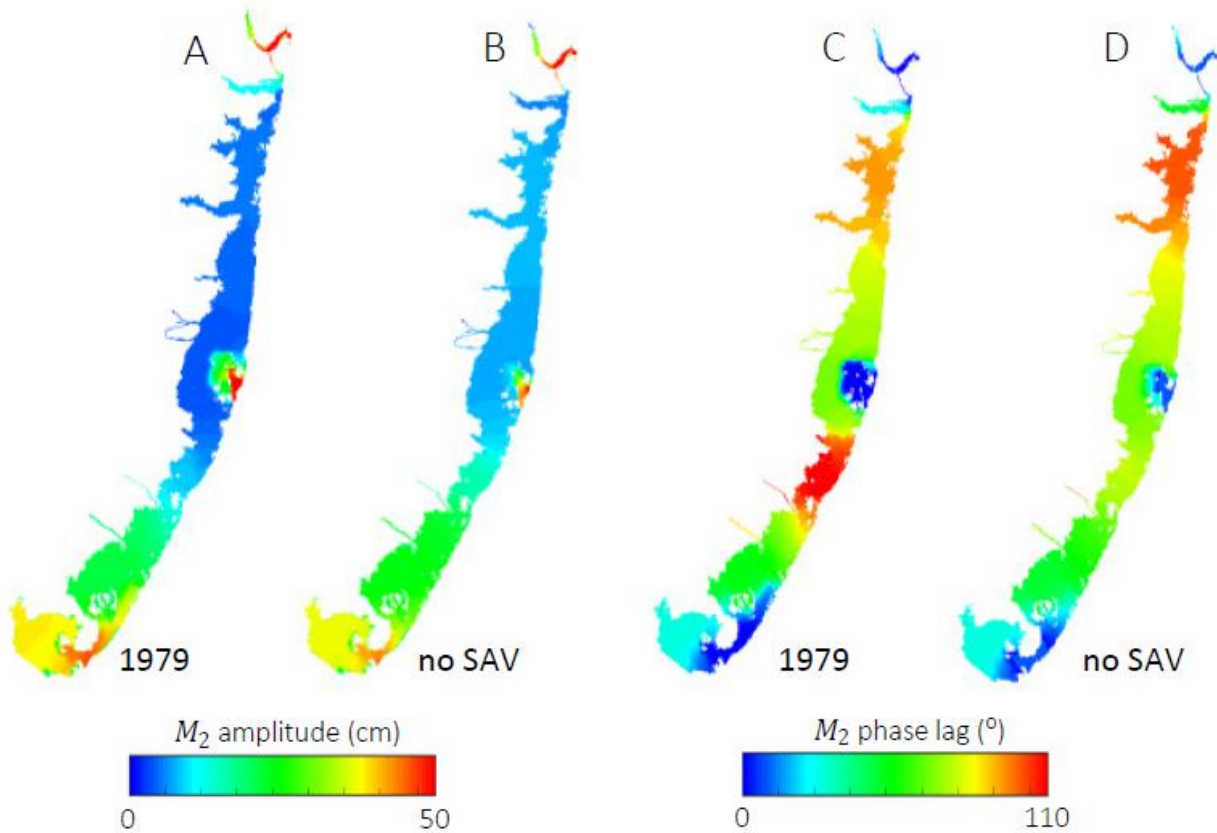
Figure 4: Sea-surface amplitude ratio and sea-surface phase of M_4 relative to M_2 for year 1979 (a, c) and no SAV case (b, d).
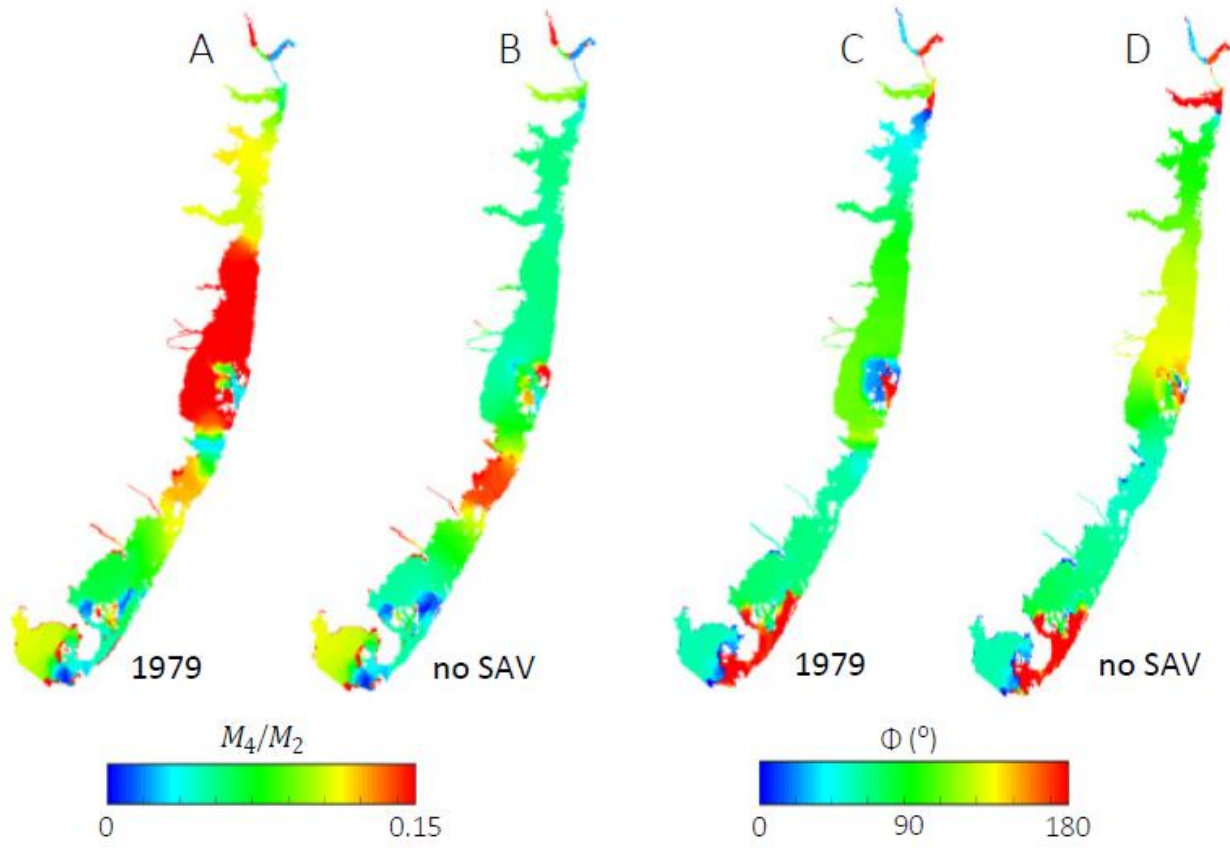
Figure 5: Mean wave height (cm) as a function of water depth (m) for a wind blowing from South-West (a) and South-East (b) with a speed of 10 m s^{-1} for three different scenarios: year 1979, year 2009 and no SAV case. Water depth data are binned every 0.3 m. Red and green areas are water depths where seagrass is present, while no seagrass is present in the white areas of the plot. Red areas are locations where seagrass presence is maximum (see Figure 2). Coloured areas do not necessary have 100% seagrass coverage.
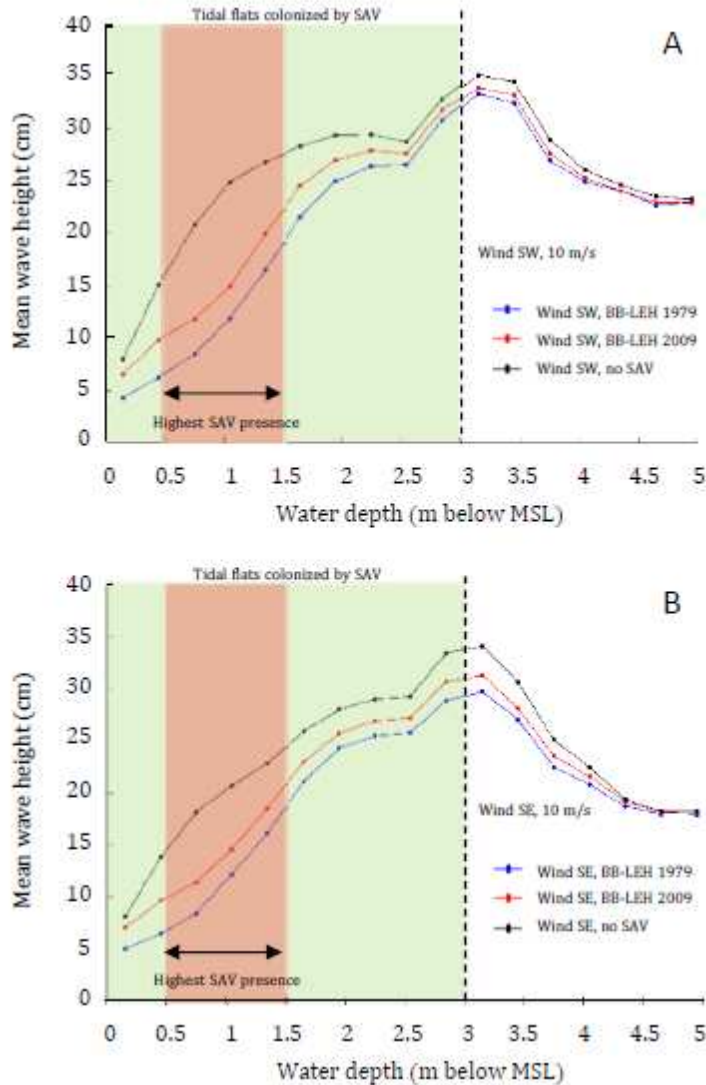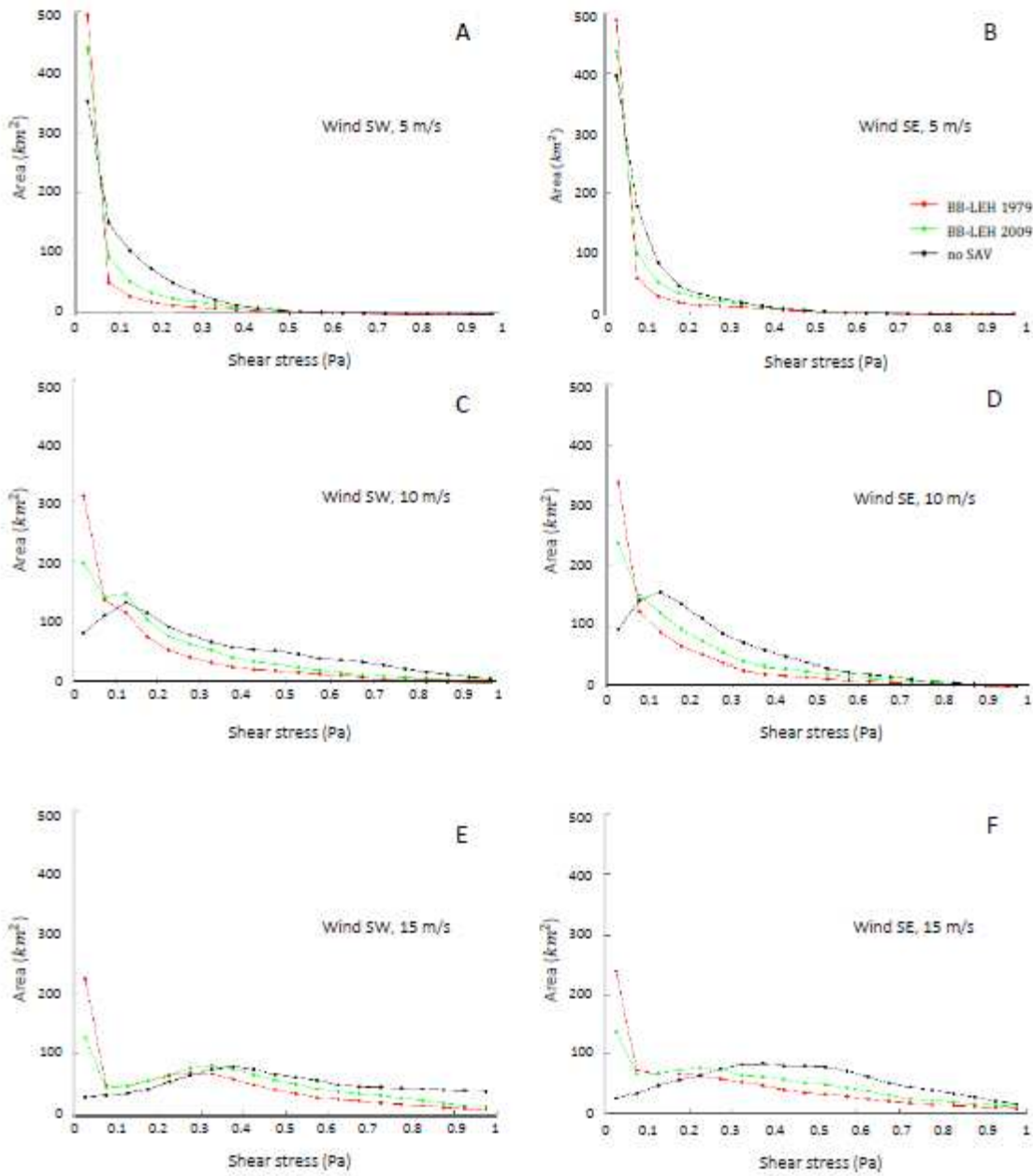
Figure 6: Mean wave height (cm) over bare beds (every depth in areas without vegetation) and meadows (every depth where seagrass meadows are present) as a function of water depth (m) for a wind blowing from South-West (a, b) and South-East (c, d) with a speed of 10 m s^{-1}.

Panels a, c refer to seagrass distribution of 1979, while panels b, d refer to seagrass distribution of 2009; differences are made with respect to the no seagrass case. Water depth data are binned every 0.3 m.
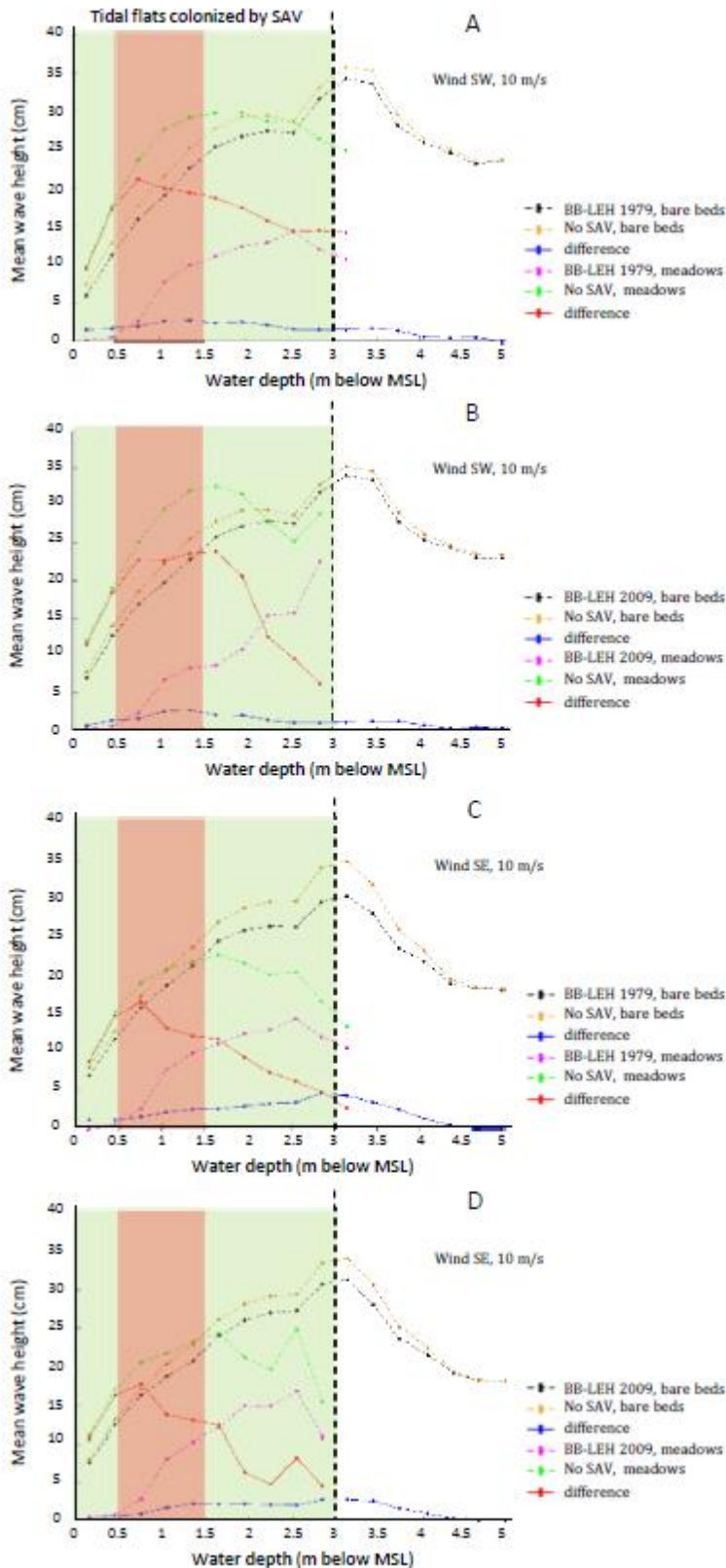
Figure 7: Distribution of shear stresses (Pa) produced by a wind of 5, 10 and 15 m s^{-1} blowing from South-West (a, c, e) and South-East (b, d, f) for three different scenarios: year 1979, year 2009 and no SAV case. Shear stress data are binned every 0.05 Pa.

Figure 8: Mean wave thrust on marsh boundary during a spring-neap cycle for a wind blowing from South-West (a) and South-East (b) with a speed of 10 m s^{-1} for two different scenarios: year 1979 and no SAV case.
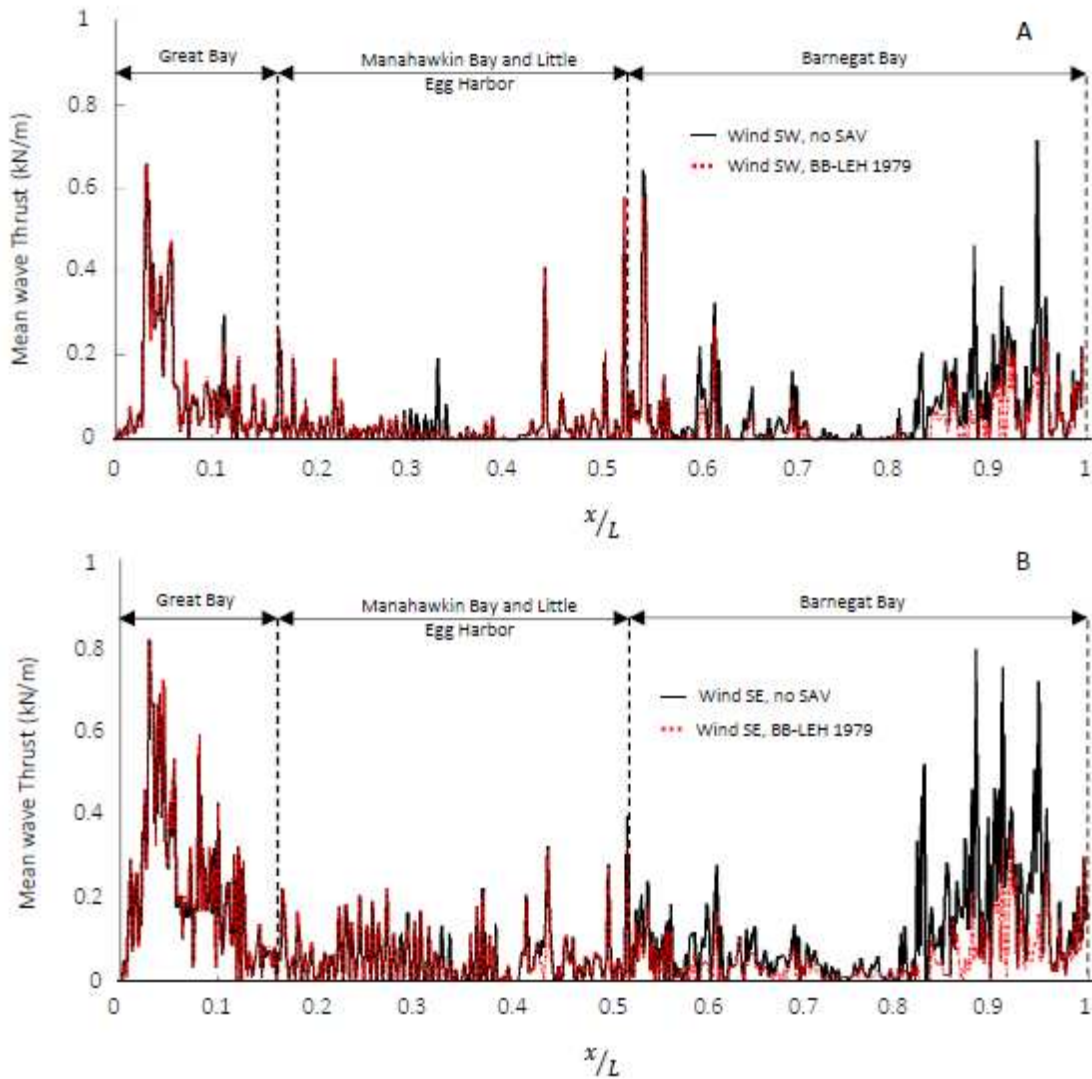
Figure 9: Decrease in wave thrust (%) with respect to no SAV case for a wind blowing from South-West (a) and South-East (b) with a speed of 5, 10 and 15 m s^{-1} in all the bay (Great Bay excluded).
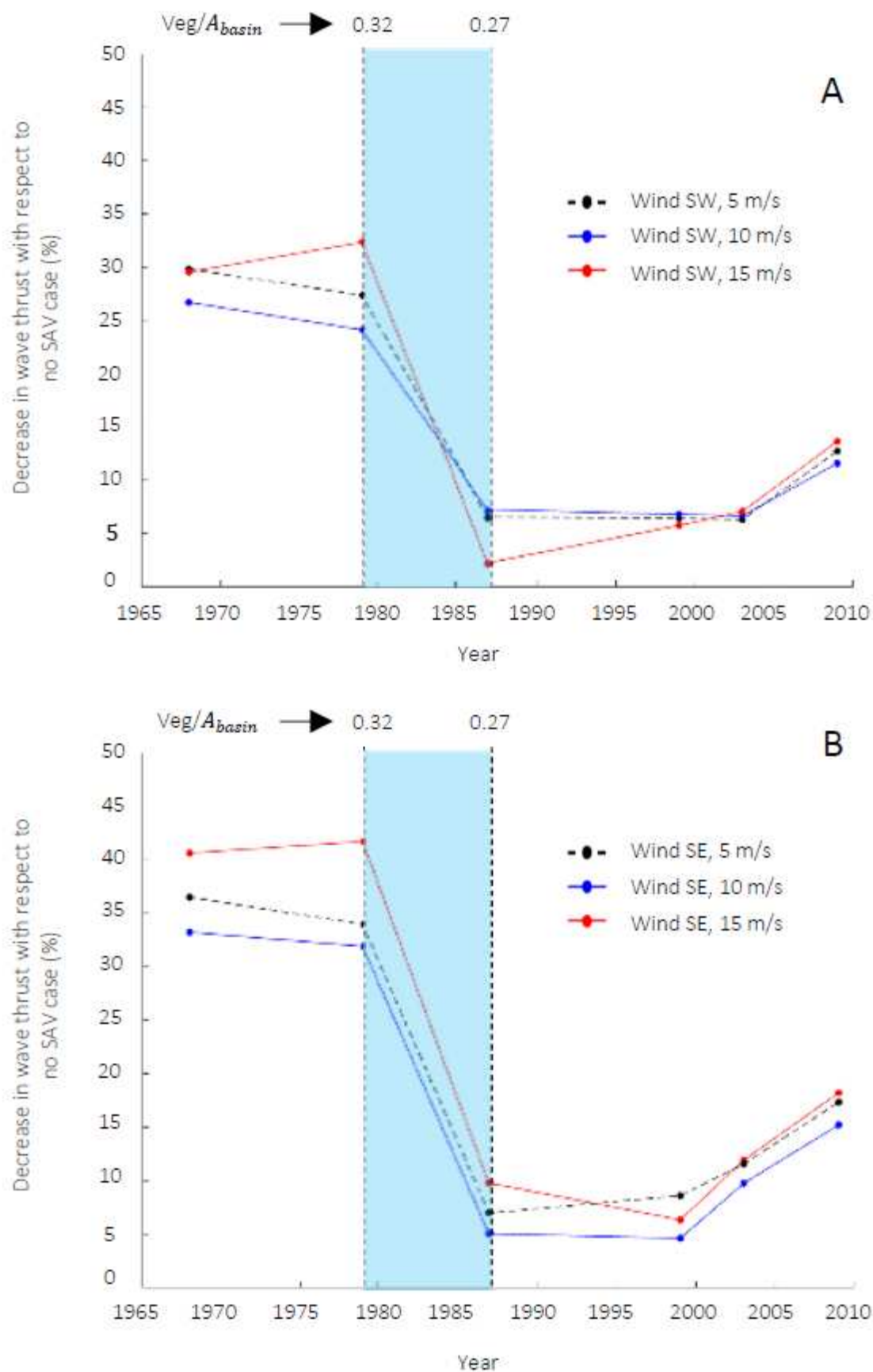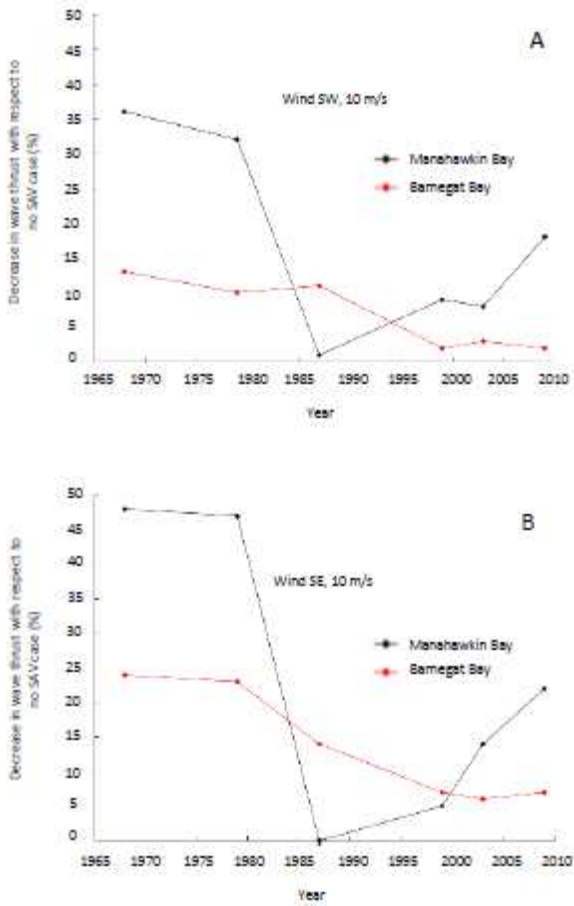
Figure 10: Decrease in wave thrust (%) with respect to no SAV case for a wind blowing from South-West (a) and South-East (b) with a speed of 10 m s^{-1} in Manahawkin Bay and Barnegat Bay.

References

Aretxabaleta, A. L., Butman, B., and Ganju, N.K., (2014). Water level response in back-barrier bays unchanged following Hurricane Sandy, Geophys. Res. Lett., 41, 3163–3171, doi:10.1002/2014GL059957.

Aubrey, D.G., and Speer, P.E., (1985). A study of non-linear tidal propagation in shallow inlet estuarine systems. Part I. Observations. Estuar. Coast. Shelf Sci. 21, 185-205.

Beudin, A., Kalra, T.S., Ganju, N.K., and Warner, J.C., (2017a). Development of a coupled wave-flow vegetation interaction model. Computers & Geosciences.

Beudin, A., Ganju, N.K., Defne, Z., and Aretxabaleta, A.L., (2017b). Physical response of a back-barrier estuary to a post- tropical cyclone. Journal of Geophysical Research: Oceans, 122, 5888–5904. https://doi.org/10.1002/2016JC012344.

Bologna, P., Lathrop, R., Bowers, P., and Able, K., (2000). Assessment of submerged aquatic vegetation in Little Egg Harbor, New Jersey. Technical Report 2000-11, Institute of Marine and Coastal Sciences, Rutgers University, New Brunswick, New Jersey, USA.

Booij, N., Ris, R.C., and Holthuijsen, L.H., (1999). A third-generation wave model for coastal regions, part I, model description and validation. Journal of Geophysical Research, C4, 7649–7666. https://doi.org/10.1029/98JC02622

Cambridge, M.L., Chiffings, A.W., Brittan, C., Moore, L., and McComb, A.J., (1986). The loss of seagrass in Cockburn Sound western Australia II; Possible causes of seagrass decline. Aquatic Botany 24: 269-286.

Cardoso, P.G., Pardal, M.A., Lillebo, A.I., Ferreira, S.M., Raffaelli, D., and Marques, J.C., (2004). Dynamic changes in seagrass assemblages under eutrophication and implications for recovery. Journal of Experimental Marine Biology and Ecology 302: 233-248.

Carr, J., Mariotti, G., Fahgerazzi, S., McGlathery, K., and Wiberg, P., (2018). Exploring the impacts of seagrass on coupled marsh-tidal flat morphodynamics. Frontiers in Environmental Science 6: 92.

Cavaleri, L., Malanotte- Rizzoli, P., (1981). Wind wave prediction in shallow water: Theory and applications, J. Geophys. Res., 86C11, 10,961–10,973.

Chapman, D. C., (1985). Numerical treatment of cross- shelf open boundaries in a barotropic coastal ocean model, J. Phys. Oceanogr., 15, 1060–1075.

Defne, Z., and Ganju, N.K., (2014). Quantifying the residence time and flushing characteristics of a shallow, back-barrier estuary: Application of hydrodynamic and particle tracking models, Estuaries Coasts, $1 - 16$, doi:10.1007/s12237-014-9885-3.

Dennison, W.C., Orth, R.J., Moore, K.A., Stevenson, J.C., Carter, V., Kollar, S., Bergstrom, P.W., Batiuk, R.A., (1993). Assessing water quality with submersed aquatic vegetation. BioScience 43: 86-94.

Dias, J. M., Lopes, J. F., and Dekeyser, I., (2000). Tidal propagation in Ria de Aveiro Lagoon, Portugal, Phys. Chem. Earth 25(4), 369–374.

Dijkstra, J., and Uittenbogaard, R., (2010). Modeling the interaction between flow and highly flexible aquatic vegetation. Water. Resour. Res. 46: W12547.

Donatelli, C., Ganju, N.K., Fagherazzi, S., and Leonardi, N., (2018a). Seagrass impact on sediment exchange between tidal flats and salt marsh, and the sediment budget of shallow bays, Geophysical Research Letters, doi:10.1029/2018GL078056.

Donatelli, C., Ganju, N.K., Zhang, X., Fagherazzi, S., and Leonardi, N., (2018b). Salt marsh loss affects tides and the sediment budget of shallow bays, Journal of Geophysical Research: Earth Surface, doi: 10.1029/2018JF004617.

Donatelli, C., Ganju, N.K., Kalra, T.S., Fagherazzi, S., and Leonardi, N., (2019). Dataset of numerical modelling results of wave thrust on salt marsh boundaries with different seagrass coverages, *Data in Brief* (published at the time article).

Dronkers, J., (1988). Coastal-offshore ecosystem. Lecture Notes on Coastal and Estuaries Studies, ed Jansson B-O (AGU, Washington, DC), Vol 22, pp 3-39.

Fagherazzi, S., (2014). Coastal processes: Storm-proofing with marshes. Nat Geosci 7(10): 701–702.

Farnsworth, E., (1998). Issues of spatial, taxonomic and temporal scale in delineating links between mangrove diversity and ecosystem function. Global Ecol Biogeogr 7 : 15–25.

Flather, R.A., (1976). A tidal model of the northwest European continental shelf, Mem. Soc. R. Sci. Liege, 6, 141–164.

Fonseca, M.S., Fisher, J.S., Zieman, J.C., and Thayer, G.W., (1982). Influence of the seagrass *Zostera marina* on current flow. Estuarine Coastal and Shelf Science 15: 351-364.

Fonseca, M.S., and Cahalan, J.A., (1992). A preliminary evaluation of wave attenuation by four species of seagrass. Estuarine, Coastal, Shelf Sci., 35: 565–576.

Fortunato, A.B., and Oliveira, A., (2005). Influence of intertidal flats on tidal asymmetry. Journal of Coastal Research 21 (5), 1062-1067.

Friedrichs, C.T., and Aubrey, D.G., (1988). Non-linear tidal distortion in shallow well-mixed estuaries: a synthesis. Estuarine Coastal and Shelf Science, 27(5), 521-545.

Gambi, M.C., Nowell, A.R. M., and Jumars, P.A., (1990). Flume observations on flow dynamics in Zostera marina eelgrass beds. Marine Ecology Progress Series 61: 159-169.

Ganthy, F., Sottolichio, A., Verney, R., (2013). Seasonal modification of tidal flat sediment dynamics by seagrass meadows of *Zostera noltii* (Bassin d'Arcachon, France). J. Mar. Syst., 109–110, pp. S233-S240.

Ganju, N.K., Defne, Z., Kirwan, M.L., Fagherazzi, S., D'Alpaos, A. and Carniello, L., (2017). Spatially integrative metrics reveal hidden vulnerability of microtidal salt marshes. Nature communications, 8, p.ncomms14156.

Ghisalberti, M., and Nepf, H.M., (2002). Mixing layers and coherent structures in vegetated aquatic flows. J. Geophys. Res. 107: 3011, doi:10.1029/2001JC000871.

Hansen, J.C. and Reidenbach, M.A., (2012). Wave and tidally driven flows in eelgrass beds and their effect on sediment suspension. Marine Ecology Progress Series, 448, pp.271-287.

Harlin, M.M., Thorne Miller, B., and Boothroyd, J.C., (1982). Seagrass sediment dynamics of a flood tidal delta in Rhode Island (USA). Aquatic Botany, 14, 127–138.

Hansen, J.C., and Reidenbach, M.A., (2013). Seasonal growth and senescence of a *Zostera marina* seagrass meadow alters wave-dominated flow and sediment suspension within a coastal bay. Estuaries and coasts, 36(6), pp.1099-1114.

Hunchak-Kariouk, K., (1999). Relation of water quality to land use in the drainage basins of four tributaries to the Toms River, New Jersey, 1994--1995. No. PB-99-149098/XAB; USGS/WRI--99-4001. Geological Survey, Water Resources Div., West Trenton, NJ (United States); New Jersey Dept. of Environmental Protection, Trenton, NJ (United States).

Joseph, J., Purdy, K., and Figley, B., (1992). The influence of water depth and bottom sediment on the occurrence of eelgrass in Barnegat, Manahawkin and Little Egg Harbor bays. Marine Fisheries Administration, New Jersey Department of Environmental Protection and Energy, Nacote Creek, New Jersey.

Kalra, T.S., Aretxabaleta, A., Seshadri, P., Ganju, N.K. and Beudin, A., (2017). Sensitivity analysis of a coupled hydrodynamic-vegetation model using the effectively subsampled quadratures method (ESQM v5. 2). Geoscientific Model Development, 10, pp.4511-4523.

Kennish, M.J., (2001). State of the estuary and watershed: an overview. Journal of Coastal Research Special Issue 32:243– 273.

Kennish, M.J., Bricker, S.B., Dennison, W.C., Glibert, P.M., Livingston, R.J., Moore, K.A., Noble, R.T., Paerl, H.W., Ramstack, J., Seitzinger, S., Tomasko, D.A., and Valiela, I., (2007a). Barnegat Bay-Little Egg Harbor Estuary: Case Study of a Highly Eutrophic Coastal Bay System. Ecological Applications 17 (Special Issue), S3-S16.

Kennish, M., Haag, S., and Sakowicz, G., (2008). Seagrass demographic and Spatial Habitat Characterization in Little Egg Harbor, New Jersey, Using Fixed Transects. Journal of Coastal Research, Special Issue 55, 148-170.

Koch, E.W., (1999). Sediment resuspension in a shallow *Thalassia testudinum* banks ex König bed. Aquatic Botany 65: 269-280.

Koch, E.W., (2001). Beyond light: Physical, geological, and geochemical parameters as possible submersed aquatic vegetation habit requirements. Estuaries 24: 1-17.

Koch, E.W., Sanford, L.P., Chen, S.-N., Shafer, D.J., and Smith, J.M., (2006). Waves in seagrass systems: review and technical recommendations. U.S. Army Corps of Engineers, Washington, DC.

Komen, G.J., Hasselmann, S., and Hasselmann, K., (1984). On the existence of a fully developed wind- sea spectrum, J. Phys. Oceanogr., 14, 1271–1285.

Lapentina, A., and Sheng, Y.P., (2014). Three-dimensional modeling of storm surge and inundation including the effects of coastal vegetation. Estuaries and Coasts, 37(4), 1028–1040. https://doi.org/10.1007/s12237-013-9730-0

Lathrop, R.G., Jr., and Bognar, J.A., (2001). Habitat loss and alteration in the Barnegat Bay Region, J. Coastal Res., 212–228, doi:10.2307/25736235.

Lathrop, R.G. and Haag, S., (2011). Assessment of Seagrass Status in the Barnegat Bay-Little Egg Harbor Estuary: 2003 and 2009. CRSSA Technical Report#2011-01. Rutgers University, Grant F. Walton Center for Remote Sensing and Spatial Analysis, New Brunswick, NJ.

Leonardi, N., and Fagherazzi, S., (2014). How waves shape salt marshes. *Geology*, *42*(10), pp.887-890.

Leonardi, N., Defne, Z., Ganju, N.K. and Fagherazzi, S., (2016a). Salt marsh erosion rates and boundary features in a shallow Bay. Journal of Geophysical Research: Earth Surface, 121(10), pp.1861-1875.

Leonardi, N., Ganju, N.K., and Fagherazzi, S., (2016b). A linear relationship between wave power and erosion determines salt-marsh resilience to violent storms and hurricanes. Proceedings of the National Academy of Sciences, 113(1), pp.64-68.

Leonardi, N., Carnacina, I., Donatelli, C., Ganju, N.K., Plater, A.J., Schuerch, M. and Temmerman, S., (2017). Dynamic interactions between coastal storms and salt marshes: A review. Geomorphology.

Macomber, R.T., and Allen, D., (1979). The New Jersey submerged aquatic vegetation distribution atlas final report. Earth Satellite Corporation, Washington, D.C.

Madsen, O.S., Poon, Y.- K., and Graber, H.C., (1988). Spectral wave attenuation by bottom friction: Theory, Proceedings of 21th International Conference on Coastal Engineering, 492–504Am. Soc. of Civ. Eng., New York.

Madsen, J.D., Chambers, P.A., James, W.F., Koch, E.W., and Westlake, D.F., (2001). The interaction between water movement, sediment dynamics and submersed macrophytes. Hydrobiologia 444: 71-84.

Marani, M., D'Alpaos, A., Lanzoni, S., and Santalucia, M., (2011). Understanding and predicting wave erosion of marsh edges, Geophys. Res. Lett., 38, L21401, doi:10.1029/2011GL048995.

Marjoribanks, T. I., Hardy, R. J., and Lane, S.N., (2014). The hydraulic description of vegetated river channels: The weaknesses of existing formulations and emerging alternatives. WIREs Water, 1(6), 549–560. https://doi.org/10.1002/wat2.1044

McCLain, P., and McHale, M., (1996). Barnegat Bay eelgrass investigations 1995–1996, p. 165–172. In G. Flimlin and M. Kennish (eds.), Proceedings of the Barnegat Bay EcosystemWorkshop. Rutgers Cooperative Extension, Toms River, New Jersey.

Mendez, F.M., and Losada, I.J., (2004). An empirical model to estimate the propagation of random breaking and nonbreaking waves over vegetation fields. Coast. Eng. 51, 103-118.

Miselis, J., Andrews, B., Baker, R., Danforth, W., DePaul, V., Defne, Z., Feinson, L., Ganju, N., Gibs, J., Hickman, R.E., Lopez, A., Navoy, A., Nicholson, R., Reilly, T., Reiser, R., Spitz, F., Watson, A., Wieben, C., and Wilson, T., (2012). Characterizing physical, chemical, and biological conditions and processes in the Barnegat Bay-Little Egg Harbor Estuary, New Jersey. 2012 Barnegat Bay Researchers Workshop, Bordentown Township, NJ.

Miselis, J.L., Andrews, B.D., Nicholson, R.S., Defne, Z., Ganju, N.K., and Navoy, A., (2015). Evolution of mid-Atlantic coastal and back-barrier estuary environments in response to a hurricane: Implications for barrier-estuary connectivity. Estuaries and Coasts. doi: 10.1007/s12237-015-0057-x.

Möller, I., Spencer, T., (2002). Wave dissipation over macro-tidal saltmarshes: Effects of marsh edge typology and vegetation change. Journal of Coastal Research, 36 (Special Issue), pp. 506-521

Moriarty, D.J.W., and Boon, P.I., (1989). Interactions of seagrass with sediment and water. In Larkum, A.W.D. and S.A. Sheppard (eds), Biology of Seagrasses. Elsevier, Amsterdam, 500-535.

Morin, J., Leclerc, M.M., Secretan, Y., and Boudreau, P., (2000). Integrated two-dimensional macrophytes-hydrodynamic modelling. Journal of Hydraulic Research, 38(3), 163–172. https://doi.org/10.1080/00221680009498334

Mukai, A.Y., Westerink, J.J., Luettich, R.A. Jr., and Mark, D., (2002). Eastcoast 2001: A tidal constituent database for the western North Atlantic, Gulf of Mexico and Caribbean Sea. US Army Engineer Research and Development Center, Coastal and Hydraulics Laboratory, Technical Report, ERDC/CHL TR-02-24.

Murray, A.B., (2007). Reducing model complexity for explanation and prediction. Geomorphology, 90 (3-4), 178-191.

Nardin, W., Larsen, L., Fagherazzi, S. and Wiberg, P., (2018). Tradeoffs among hydrodynamics, sediment fluxes and vegetation community in the Virginia Coast Reserve, USA. *Estuarine, Coastal and Shelf Science*.

Nepf, H., (2012). Flow and transport in regions with aquatic vegetation. Ann. Rev. Fluid Mech., 44: 123–142.

NOAA NOS. (2012). National Ocean Service Hydrographic Survey data, National Oceanic and Atmospheric Administration, http://www.ngdc.noaa.gov/mgg/bathymetry/hydo.html. Accessed 2012.

Nowacki, D.J., Beudin, A., and Ganju, N.K., (2017). Spectral wave dissipation by submerged aquatic vegetation in a back-barrier estuary. Limnol. Oceanogr., 62 (2), pp. 736-753

Orlanski, I., (1976), A simple boundary condition for unbounded hyperbolic flows, J. Comp. Sci., 21(3), 251–269.

Orth, R.J., Luckenbach, M.L., Marion, S.R., Moore, K.A., and Wilcox, D.J., (2006). Seagrass recovery in the Delmarva Coastal Bays, USA. Aquatic Botany 84: 26-36.

Peterson, C.H., Luettich, R.A., Micheli, F., and Skilleter, G.A., (2004). Attenuation of water flow inside seagrass canopies of differing structure. Mar. Ecol. Prog. Ser., 268, pp. 81-92.

Paul, M., and Amos, C.L., (2011). Spatial and seasonal variation in wave attenuation over *Zostera noltii.* J. Geophysical Research 116, C09019.

Pawlowicz, R., Beardsley, B., and Lentz, S., (2002). Classical tidal harmonic analysis including error estimates in MATLAB using T_TIDE, Comput. Geosci., 28, 929–937.

Picado, A., Dias, J.M., and Fortunato, A.B., (2010). Tidal changes in estuarine systems induced by local geomorphologic modifications. Continental Shelf Research, 30 (17), pp. 1854-1864, 10.1016/j.csr.2010.08.012.

Potouroglou, M., Bull, J.C., Krauss, K.W., Kennedy, H.A., Fusi, M., Daffonchio, D., Mangora, M.M., Githaiga, M.N., Diele, K., and Huxham, M., (2017). Measuring the role of seagrasses in regulating sediment surface elevation. Scientific Report, doi:10 .1038/s41598-017-12354-y.

Preen, A.R., Long, W.-J.L., and Coles, R.G., (1995). Flood and cyclone related loss, and partial recovery, of more than 1000 km^2 of seagrass in Hervey Bay. Queens-land, Australia. Aquatic Botany 52: 3-17.

Priestas, A.M., Mariotti, G., Leonardi, N., and Fagherazzi, S., (2015). Coupled wave energy and erosion dynamics along a salt marsh boundary, Hog Island Bay, Virginia, USA. Journal of Marine Science and Engineering, 3(3), pp.1041-1065.

Schwimmer, R., (2001). Rates and processes of marsh shoreline erosion in Rehoboth Bay, Delaware, U.S.A., J. Coastal Res., 17(3), 672-683, doi:10.1016/j.csr.2009.08.018.

Short, F.T and Burdick, D.B., (1996). Quantifying eelgrass habit loss in relation to housing development and nitrogen loading in Waquoit Bay, Massachusetts. Estuaries 19: 730-739.

Suzuki, T., Zijlema, M., Burger, B., Meijer, M.C., and Narayan, S., (2012). Wave dissipation by vegetation with layer schematization in SWAN. Coast. Eng. 59 (1), 64-71.

Temmerman, S., Meire, P., Bouma, T.J., Herman, P.M., Ysebaert, T., and De Vriend, H.J., (2013). Ecosystem-based coastal defence in the face of global change. Nature 504 (7478): 79–83. https://doi.org/10. 1038/nature12859.

Terrados, J. and Duarte, C.M., (2000). Experimental evidence of reduced particle resuspension within a seagrass (*Posidonia oceanica* L.) meadow. Journal of Experimental Marine Biology and Ecology 243: 45-53.

Tommasini, L., Carniello, L., Ghinassi, M., Roner, M., and D'Alpaos, A., (2019). Changes in the wind-wave field and related salt-marsh lateral erosion: interferences from the evolution of the Venice Lagoon in the last four centuries, Earth Surface Processes and Landforms, doi:10.1002/esp.4599.

Tonelli, M., Fagherazzi, S., and Petti, M., (2010). Modeling wave impact on salt marsh boundaries, J. Geophys. Res., 115, C09028, doi:10.1029/2009JC006026.

U.S. Army Corps of Engineers, (1976). Aquatic Plant Control Project for the State of New Jersey: Design Memorandum No.1. Philadelphia District, Philadelphia, Pennsylvania.

Warner, J.C., Armstrong, B., He, R., and Zambon, J.B., (2010). Development of a coupled ocean-atmosphere-wave-sediment transport (COAWST) modeling system. Ocean Model., 35 (3), pp. 230-244.

Waycott, M., Duarte, C.M., Carruthers, T.J.B., Orth, R.J., Dennison, W.C., et al. (2009). Accelerating loss of seagrasses across the globe threatens coastal ecosystems. Proc. Natl. Acad. Sci. USA 106:12377-81.